ResearchGate

See discussions, stats, and author profiles for this publication at: https://www.researchgate.net/publication/7846794

# Computations on the Ã–X̃ transition of isoprene–OH–O2 peroxy radicals

**ARTICLE** *in* JOURNAL OF COMPUTATIONAL CHEMISTRY · JUNE 2005

Impact Factor: 3.59 · DOI: 10.1002/jcc.20216 · Source: PubMed

CITATIONS
2

READS
38

**1 AUTHOR:**

Theodore S Dibble
State University of New York College of Env…

**79** PUBLICATIONS **1,026** CITATIONS

SEE PROFILE

Available from: Theodore S Dibble
Retrieved on: 25 January 2016

# Computations on the $\tilde{A}$–$\tilde{X}$ Transition of Isoprene-OH-$O_2$ Peroxy Radicals

**THEODORE S. DIBBLE**
*Chemistry Department, State University of New York–Environmental Science and Forestry, 1 Forestry Drive, Syracuse, New York 13210*

*Received 10 December 2004; Accepted 29 January 2005*
*DOI 10.1002/jcc.20216*
*Published online in Wiley InterScience (www.interscience.wiley.com).*

**Abstract:** Calculations are carried out on the $\tilde{A}$ state of $HO_2$, $CH_3O_2$, and $CH_3CH_2O_2$ and 10 isomers and conformers of the isoprene-OH-$O_2$ peroxy radicals derived from OH addition to isoprene (2-methyl-1,3-butadiene). In addition to calculating vertical and adiabatic excitation energies, we consider the effect of excitation on molecular structure, and examine the OO stretching frequencies, which are known to be major features in the absorption spectra of the $\tilde{A}$ states of the smaller radicals. The two methods used are the configuration interaction with single excitations (CIS) method and time-dependent density functional theory (TD-DFT), both with a range of basis sets up to 6-311++G(2df,2pd). TD-DFT overestimates excitation energies considerably, while CIS tends to underestimate them slightly. TD-DFT does seem to capture the trend in excitation energy vs. size for the smaller peroxy radicals. Conformation and configuration strongly affect the excitation energies of the peroxy radicals from isoprene. CIS calculations indicate that the intramolecular OH—O hydrogen bonds, present in the ground state of some peroxy radicals from isoprene, are weakened or broken in the excited state, while TD-DFT calculations suggest they are retained.

© 2005 Wiley Periodicals, Inc. J Comput Chem 26: 836–845, 2005

**Key words:** peroxy radicals; electronic spectroscopy; time-dependent density functional theory; isoprene; hydrogen bonding

## Introduction

Organic peroxy radicals, $RO_2$, are critical intermediates in combustion and atmospheric chemistry. Their reactions in the lower atmosphere can propagate ozone-forming catalytic cycles or terminate those same cycles.[1,2] Via their isomerization to QOOH radicals, organic peroxy radicals influence the occurrence of autoignition ("knocking") in internal combustion engines.[3,4] The reaction kinetics of these radicals have been the subject of much study, and most real-time kinetic studies have used the strong ~250 nm absorption of the $\tilde{B}$–$\tilde{X}$ transition to determine peroxy radical concentration.[1,2] Unfortunately, the $\tilde{B}$ state is dissociative, so this transition consists of a single broad peak lacking in vibrational structure; furthermore, the vertical transition energy is nearly independent of the nature of the organic moiety.[1,5,6] These factors make it difficult or impossible to use this transition to simultaneously monitor the concentration of two different organic peroxy radicals. To avoid this difficulty, some groups have turned to chemical ionization mass spectrometry[7,8] or mid-infrared spectroscopy as analytical tools.[9] In addition, several groups have begun taking advantage of the sensitivity of cavity ringdown spectroscopy (CRDS) to monitor peroxy radicals via their $\tilde{A}$–$\tilde{X}$ transition in the near-infrared (NIR).[10–13] The $\tilde{A}$-$\tilde{X}$ transition exhibits vibrational structure, and may be suited for monitoring specific organic peroxy radicals in the presence of other peroxy radicals. Moreover, it has been suggested that absorption of NIR photons by peroxy radicals could occur at rates competitive with the bimolecular reactions that are currently thought to control the fate of these radicals.[14]

This article is aimed at testing the reliability of excited state methods for treating the $\tilde{A}$–$\tilde{X}$ transition of peroxy radicals derived from isoprene (2-methyl-1,3-butadiene). Isoprene is an extremely important source of peroxy radicals in the lower atmosphere. Approximately 500 *Tg* of isoprene are emitted to the atmosphere each year,[15] and the OH-radical initiated degradation of isoprene produces eight peroxy radical isomers (isoprene-OH-$O_2$), as shown in Figure 1.[16,17] Uncertainties surrounding the chemistry of these radicals contribute significantly to discrepancies between model predictions and field measurements of peroxy radical concentration,[18,19] and to uncertainties in models of ozone production

***Correspondence to:*** T.S. Dibble; e-mail: tsdibble@syr.edu

Contract/grant sponsor: the National Science Foundation; contract/grant numbers: ATM-0087057 and ATM-0352926

© 2005 Wiley Periodicals, Inc.

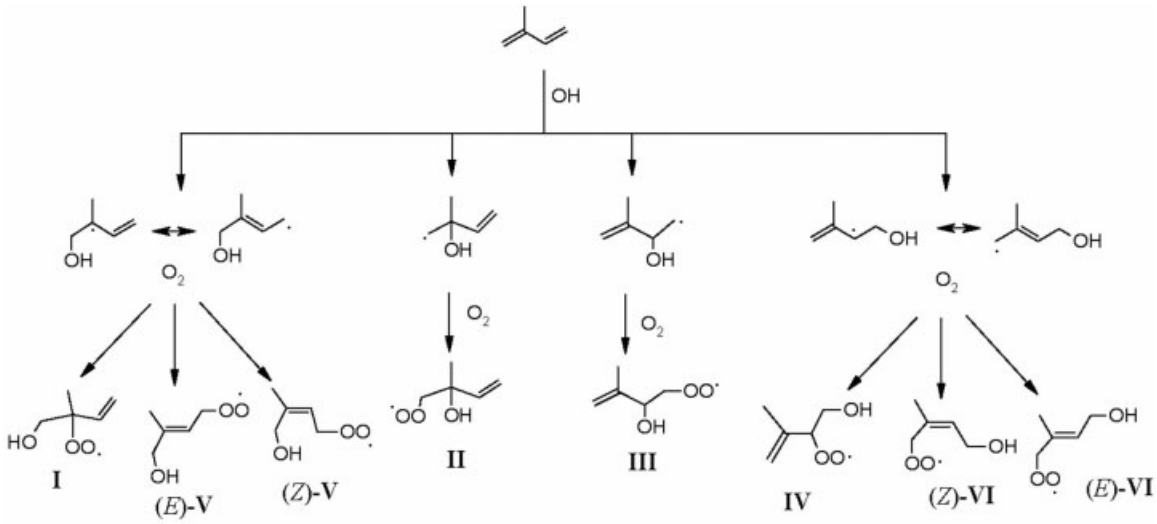


**Figure 1.** Sketches of the reactions forming the eight isomeric isoprene-OH-$O_2$ peroxy radicals.

in polluted air.[20] There is great interest in using CRDS in the NIR to monitor the concentrations of the isoprene-OH-$O_2$ radicals in kinetics experiments. To support these experimental efforts, we have carried out computations on all eight isomers of these isoprene-OH-$O_2$ radicals, as well as $HO_2$, $CH_3O_2$, and $CH_3CH_2O_2$.

Below we present the computational methods employed. We then discuss the structures of the radicals, their vertical and adiabatic excitation energies, and their OO vibrational frequencies in the excited state. There have been a number of experimental studies of the Ã–X̃ transition in small peroxy radicals, including $HO_2$,[21–25] $CH_3O_2$,[21,26] and $CH_3CH_2O_2$,[21,26] which provide data we use to evaluate the reliability of the methods employed here and their potential to interpret experimental studies of the isoprene-OH-$O_2$ radicals.

## Computational Methods

Quantum chemical computations were carried out using the GAUSSIAN98[27] series of programs. Initial structures of the ground states of $HO_2$,[28] $CH_3O_2$,[29] and the *trans* and *gauche* conformers of $CH_3CH_2O_2$,[29,30] were obtained from the literature. Ground-state geometries were then optimized using the hybrid exchange functional of Becke[31] combined with the correlation functional of Lee, Yang, and Parr,[32] a combination denoted B3LYP, together with the 6-31G(d,p) basis set. This combination of method and basis set has been shown to do a very good job at predicting molecular structures of radicals.[33] All species were treated with the spin-unrestricted formalism. B3LYP/6-31G(d,p) structures for most of the isoprene-OH-$O_2$ radicals, including the (E) isomers of **V** and **VI** (see Fig. 1), were provided by Zhang.[34] Initial structures of the (Z) isomers of **V** and **VI** were obtained by rotating one end of the radicals by 180 degrees. The orientation of the terminal —$CH_2$OH group was then set to produce both hydrogen bonded and nonhydrogen bonded conformers of the (Z) isomers of **V** and **VI**. These structures were then optimized at B3LYP/6-31G(d,p). Harmonic vibrational frequencies of the ground states of all species were obtained at B3LYP/6-31G(d,p) to verify that the structures were potential energy minima.

Excited states were studied using the configuration interaction-singles (CIS) method and time-dependent density functional theory (TD-DFT).[35–38] TD-DFT calculations used the B3LYP functional. To determine vertical excitation energies, single-point calculations were carried out at the ground-state geometries of all species using three basis sets: 6-31+G(d,p), 6-311++G(d,p), 6-311++G(2d,2p). In addition, the 6-311++G(2df,2pd) basis set was employed for $HO_2$, $CH_3O_2$, and the *trans* and *gauche* conformers of $CH_3CH_2O_2$.

The structures of the Ã states of the radicals were determined using the CIS method. Although CIS is not the best method for excited states,[39,40] determining excited state structures and vibrational frequencies of asymmetric radicals as large as the isoprene-OH-$O_2$ species is prohibitively expensive using more reliable methods. For $HO_2$, $CH_3O_2$, and the *trans* and *gauche* conformers of $CH_3CH_2O_2$, the geometry and harmonic vibrational frequencies of the Ã state were determined at each of the four basis sets listed above. Due to the large size of the isoprene-OH-$O_2$ radicals, their excited state geometries and harmonic vibrational frequencies were only determined at CIS/6-31+G(d,p). Adiabatic excitation energies of all species were computed from the vertical excitation energies by subtracting the differences between the absolute CIS energies of the Ã state at the X̃ and Ã state geometries.

## Results and Discussion

Figure 2 shows the molecular structure of the smaller radicals, with key bond lengths and angles listed for the ground and excited state. $CH_3CH_2O_2$ exists in two conformers, *gauche* and *trans*, relative energies of which have been extensively studied.[30] Our B3LYP results agree with previous studies indicating that the *gauche* conformer is the slightly more stable conformer (by 0.2 kcal/mol).

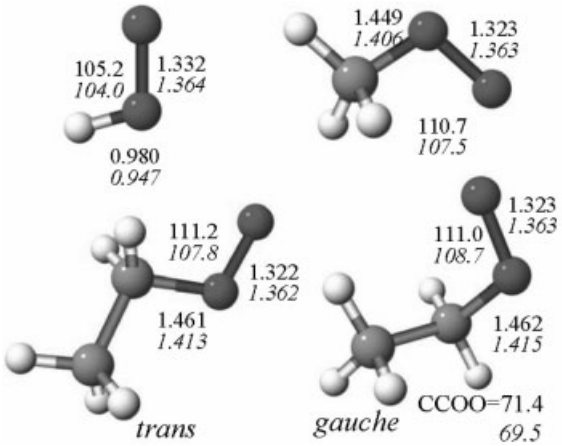


**Figure 2.** Molecular structures of small peroxy radicals, showing critical distances in Angstroms and angles in degrees: ground state values [at B3LYP/6-31G(d,p)] are listed above the CIS/6-311++G(2df,2pd) values for the $\tilde{A}$ state (in italics). For $CH_3O_2$ and $CH_3CH_2O_2$, only the CO and OO distances and the COO angle are presented.

The small energy difference between the two conformers implies that both are present in comparable amounts at room temperature, where most experimental studies have been carried out.

As can be seen from Table 1, the computed geometries of the excited states are mostly independent of basis set, especially if one excludes the results of the smallest basis set [6-31+G(d,p)]. To determine the effect of geometry on the *energy* of the $\tilde{A}$ state, a series of single point calculations was carried out for the $CH_3O_2$ radical at the CIS/6-31+G(d,p) geometry using the three larger basis sets. These calculations showed that the small geometry differences noted in Table 1 have minimal effects (12–32 $cm^{-1}$) on the computed CIS energy. Considering the small affects of basis set on molecular structure and the inherent error in CIS calculations, these results suggest that geometry calculations on excited states of larger peroxy radicals need not use a basis set larger than 6-31+G(d,p).

As can be seen from Figures 3 and 4, the most obvious effect of electronic excitation on the molecular structure of the isoprene-OH-$O_2$ radicals is the weakening or breaking of the hydrogen bonds. The modest reduction in covalent O—H bond lengths does not appear to result from the weakening of the hydrogen bonds, because it occurs in conformers and isomers whose ground states did not possess hydrogen bonds. Note that hydrogen bonded and non-hydrogen bonded conformers of the (*Z*) isomers of **V** and **VI** are labeled "H" and "nonH," respectively, in the figures and tables. Figure 5 shows the dependence of the electronic energy on the covalent OH distance in the non-hydrogen bonded conformer of (*Z*)-**V**, in both the $\tilde{A}$ and $\tilde{X}$ states, with all other geometrical parameters frozen at the $\tilde{A}$ values. Figure 5 displays the values from B3LYP/6-31+G(d,p), but the corresponding curves using the 6-31G(d,p) data are almost indistinguishable. It is clear from Figure 5 that the equilibrium value of the OH bond length is very nearly the same in the $\tilde{X}$ state as in the $\tilde{A}$ state. Therefore, the apparent reduction in the covalent OH distance seen in Figures 3 and 4 is an artifact of comparing DFT and CIS geometries.

The marked difference between the CIS and DFT geometries motivated a scan of the potential energy of the $\tilde{A}$ state of $HO_2$ and $CH_3O_2$ using TD-DFT and the 6-311+G(d,p) basis set. The $\tilde{A}$ state geometry of $HO_2$ was completely optimized, while for $CH_3O_2$ only the C—O and O—O bond lengths and the COO angle were optimized (other parameters were constrained to the ground state values). The optimization was initiated with a coarse grid search, following which the minimum energy structure was determined on a grid that had bond length intervals of 0.0003 Å and angle intervals of 0.05 degrees; this provides an accuracy compa-

**Table 1.** Critical Geometric Parameters of the $\tilde{A}$ State of $HO_2$, $CH_3O_2$, and the *trans* and *gauche* Conformers of $CH_3CH_2O_2$ Using CIS with Various Basis Sets (Distances in Angstroms, Angles in Degrees).

| Species | Basis set | OH/CO | OO | HOO/COO |
|---|---|---|---|---|
| HOO ($^2A'$) | 6-31+G(d,p) | 0.950 | 1.376 | 105.6 |
| | 6-311+G(d,p) | 0.948 | 1.364 | 103.9 |
| | 6-311++G(2d,2p) | 0.946 | 1.369 | 103.8 |
| | 6-311++G(2df,2pd) | 0.947 | 1.364 | 104.0 |
| $CH_3O_2$($^2A'$) | 6-31+G(d,p) | 1.411 | 1.376 | 107.1 |
| | 6-311+G(d,p) | 1.409 | 1.363 | 107.6 |
| | 6-311++G(2d,2p) | 1.408 | 1.369 | 107.2 |
| | 6-311++G(2df,2pd) | 1.406 | 1.363 | 107.5 |
| *trans* $CH_3CH_2O_2$ ($^2A''$) | 6-31+G(d,p) | 1.418 | 1.375 | 107.4 |
| | 6-311+G(d,p) | 1.417 | 1.363 | 108.0 |
| | 6-311++G(2d,2p) | 1.415 | 1.368 | 107.5 |
| | 6-311++G(2df,2pd) | 1.413 | 1.362 | 107.8 |
| *gauche* $CH_3CH_2O_2$ ($C_1$) | 6-31+G(d,p) | 1.420 | 1.377 | 108.2 |
| | 6-311+G(d,p) | 1.418 | 1.364 | 108.7 |
| | 6-311++G(2d,2p) | 1.417 | 1.369 | 108.4 |
| | 6-311++G(2df,2pd) | 1.415 | 1.363 | 108.7 |

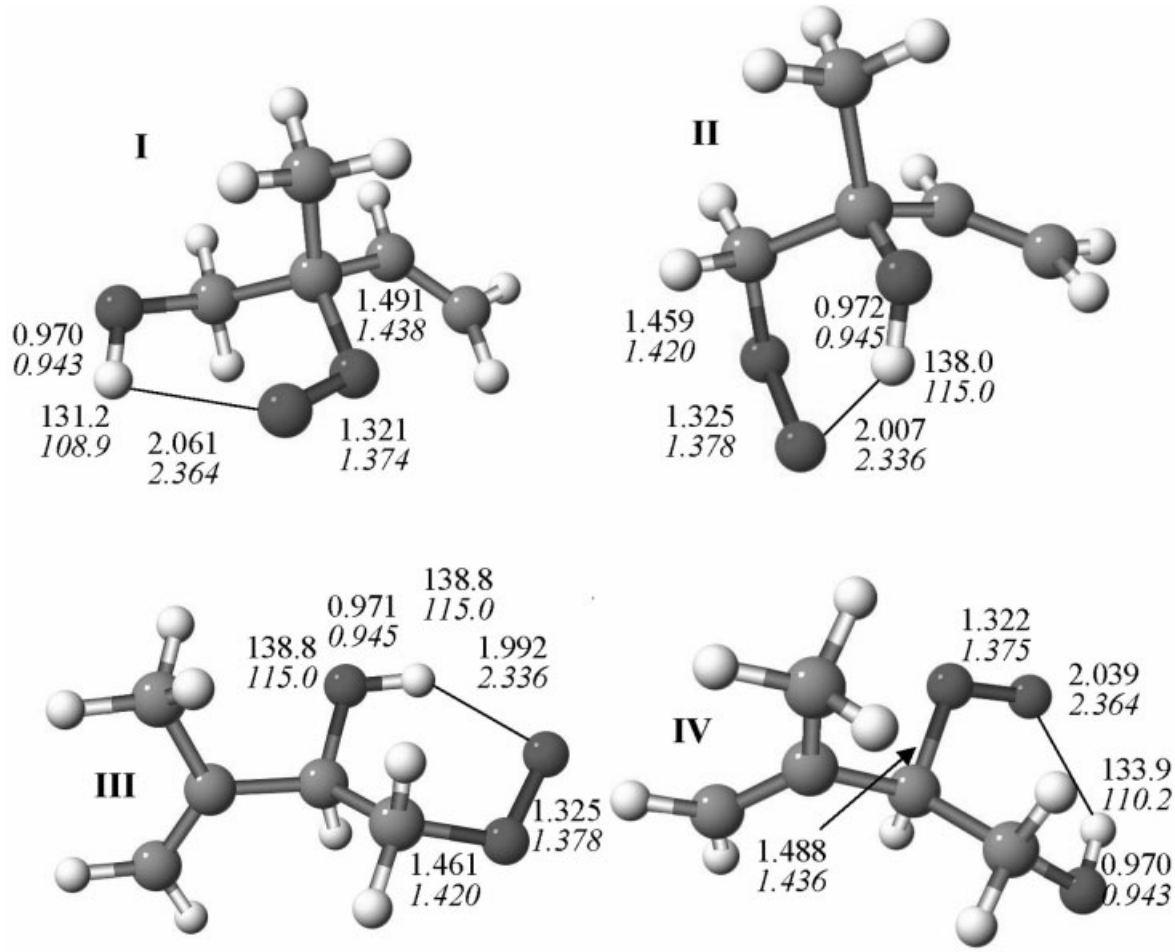


**Figure 3.** Molecular structures of peroxy radicals **I–IV** from isoprene, showing critical distances in Angstroms and angles in degrees: ground-state values [at B3LYP/6-31G(d,p)] are listed above the CIS/6-31+G(d,p) values for the Ã state (in italics). The only distances presented are the covalent CO, OO, and OH bond lengths along with the hydrogen bonded OH–O distances. The only angles listed are the valence COO angle and the OH–O hydrogen bond angle.

rable to that obtained in the other geometries reported here. The computed results at CIS and TD-DFT are listed side by side in Table 2, along with the previously published experimental[41] and MR-CISD[42] results for $HO_2$. The comparison suggests that TD-DFT is performing somewhat better than CIS, but neither of the methods used here captures the full effect of electronic excitation on the length of the OO bond. In addition, the HOO angle calculated at TD-DFT (and MR-CISD) is worse than the CIS value.

For $CH_3O_2$, the computed OO bond lengths agree well between the two methods. For both $HO_2$ and $CH_3O_2$, the valence angle involving the peroxy group (HOO or COO) is somewhat larger at TD-DFT than at CIS, and TD-DFT predicts H–OO/C–OO distances about 2% larger than the CIS values.

Table 3 lists vertical excitation energies for $HO_2$, $CH_3O_2$, and the *trans* and *gauche* conformers of $CH_3CH_2O_2$, while Table 4 lists computed adiabatic excitation energies along with experimental values. Because of the uncertainty in scaling the zero-point energy of the CIS calculations, we have not corrected for differences in zero-point energies of the ground and excited states. The available experimental data suggest that, in the case of $HO_2$, correcting for zero point energies lowers the computed adiabatic excitation energy by only $\sim$210 $cm^{-1}$.

The values from Tables 3 and 4 are plotted in Figures 6–8. The adiabatic transition energies from CIS agree better with experiment than the TD-B3LYP results, which are generally much too high (note that experimental results for $CH_3CH_2O_2$ have not been assigned to a particular conformer). However, the CIS results, unlike the TD-DFT results, are strongly dependent on basis set, and no one basis set performs consistently well. The MR-CISD/DZP calculation cited earlier for $HO_2$ give a vertical excitation energy of 7580 $cm^{-1}$, which would be reduced to about 7250 $cm^{-1}$ (vs. 7030 $cm^{-1}$ from experiment) by including the theoretical zero-point energies. The CIS/6-31+G(d,p) calculations consistently underestimate the adiabatic transition energies even without accounting for the effects

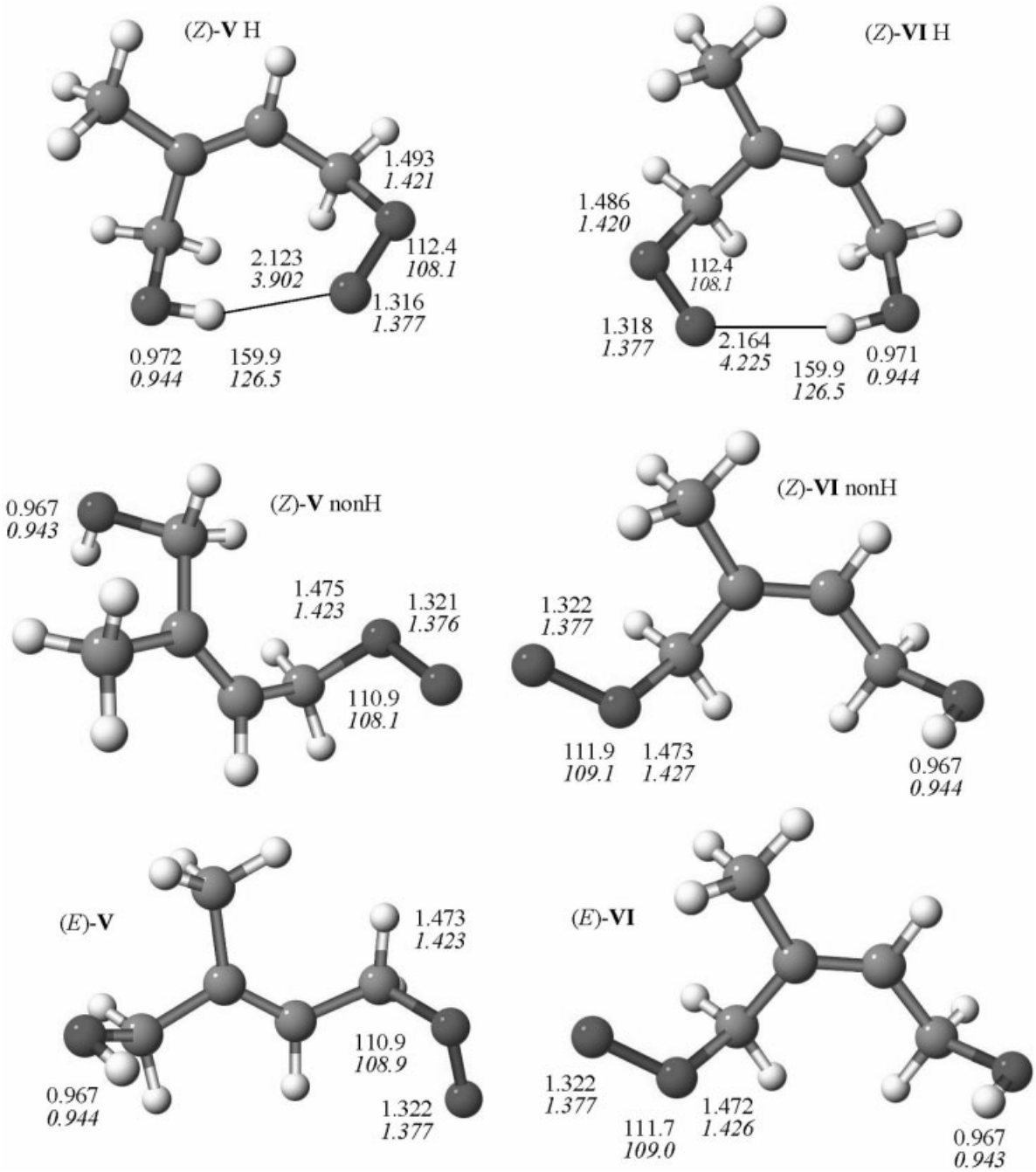


**Figure 4.** Molecular structures of isomers and conformers of peroxy radicals **V** and **VI** from isoprene, showing critical distances in Angstroms and angles in degrees: ground-state values [at B3LYP/6-31G(d,p)] are listed above the CIS/6-31+G(d,p) values for the $\tilde{A}$ state (in italics). The only distances presented are the covalent CO, OO, and OH bond lengths along with hydrogen bonded OH–O distances. The only angles listed are the valence COO angles and OH–O hydrogen bond angles.

of zero-point energy: by 300 $cm^{-1}$ for $HO_2$ and rising to 1000 $cm^{-1}$ for $CH_3CH_2O_2$.

Similar differences between TD-DFT and CIS vertical excitation energies were found by Weisman and Head–Gordon for $HO_2$ and $CH_3O_2$.[6] As in the present work, they used B3LYP for the ground-state geometry and TD-DFT calculations, and used 6-31+G(d,p) basis sets for computing excitation energies. Their values of the vertical excitation energies of $HO_2$ and $CH_3O_2$ are

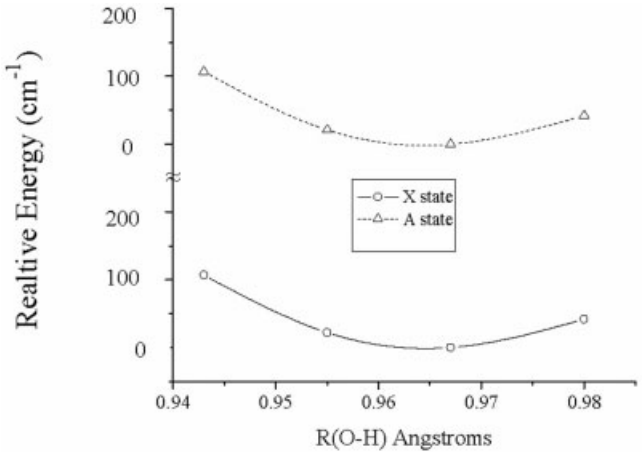


**Figure 5.** Relative electronic energy ($cm^{-1}$) vs. covalent OH distance for the ground and Ã states of non-hydrogen bonded conformer of (*Z*)-**V** at B3LYP/6-31+G(d,p), with all other geometric parameters frozen. The lines are cubic spline fits.

roughly 2000 $cm^{-1}$ (ROCIS) and 4000 $cm^{-1}$ (XCIS) lower than the UCIS values reported here.

The CIS results fail to account for the experimentally observed increase in the adiabatic excitation energy with increasing size of the group attached to the radical ($H < CH_3 < C_2H_5$). The TD-DFT results do seem to capture the trend and even its magnitude, especially if one focuses on the more stable *gauche* conformer of $C_2H_5O_2$ rather than the *trans* conformer. The computed vertical (adiabatic) excitation energies of the *gauche* conformer are consistently 162–166 (178–195) $cm^{-1}$ higher than those of the *trans* conformer at all four basis sets. These differences are greater than the computed energy difference of the ground state, which is only 30–100 $cm^{-1}$ (depending on the level of theory).[29,30]

The small affect of the nature of the R group on computed excitation energies of ROO radicals (which is in accord with experiment) was explained by Weisman and Head–Gordon.[6] They pointed out that this transition is of a $\beta$ electron from the highest doubly occupied molecular orbital (HOMO) to the singly occupied molecular orbital (SOMO), and the energies of both orbitals are nearly independent of the nature of the R group, even for R = phenyl or vinyl.

Table 5 lists the CIS values of the vertical and adiabatic excitation energies of the isoprene-OH-$O_2$ radicals, while Table 6 lists the TD-DFT results. The range of molecular structures and

**Table 2.** Geometries (Distances in Angstroms, Angles in Degrees) of the $\tilde{A}^2A'$ State of $HO_2$ and $CH_3O_2$ Radicals at the 6-311+G(d,p) Basis Set, Together with Literature Results for $HO_2$.

| | $HO_2$ | | | | $CH_3O_2$ | |
|---|---|---|---|---|---|---|
| Parameter | CIS | TD-DFT | MR-CISD/DZP[a] | exp[b] | CIS | TD-DFT |
| OO | 1.364 | 1.376 | 1.41 | 1.393 | 1.363 | 1.362 |
| HO/CO | 0.948 | 0.967 | 0.975 | 0.965 | 1.409 | 1.436 |
| HOO/COO | 103.9 | 104.4 | 104.8 | 102.7 | 107.6 | 108.9 |

Note that for TD-DFT optimizations of $CH_3O_2$, only the listed parameters were optimized.
[a]Ref. 42.
[b]Ref. 41.

**Table 3.** CIS and TD-DFT Vertical Excitation Energies ($cm^{-1}$) of the $\tilde{A}$ States of Small Peroxy Radicals.

| | $HO_2$ | | $CH_3O_2$ | | *trans* $CH_3CH_2O_2$ | | *gauche* $CH_3CH_2O_2$ | |
|---|---|---|---|---|---|---|---|---|
| Basis set or method | CIS | DFT | CIS | DFT | CIS | DFT | CIS | DFT |
| 6-31+G(d,p) | 7269 | 8956 | 7347 | 9286 | 7372 | 9250 | 7534 | 9452 |
| 6-311+G(d,p) | 7071 | 8913 | 7155 | 9219 | 7176 | 9182 | 7339 | 9386 |
| 6-311++G(2d,2p) | 7524 | 9003 | 7599 | 9313 | 7615 | 9266 | 7780 | 9484 |
| 6-311++G(2df,2pd) | 7880 | 9077 | 7939 | 9377 | 7954 | 9331 | 8120 | 9548 |
| CASSCF/cc-VTZ | 8644[a] | | | | | | | |
| MRCISD/cc-VTZ | 8039[a,b] | | | | | | | |
| MRCI/DZP | 8230[c] | | 7270[d] | | | | | |

[a]Ref. 43.
[b]Based on CASSCF wave function of ref. 43.
[c]Ref. 42.
[d]Ref. 44.

**Table 4.** CIS and TD-DFT[a] Adiabatic Excitation Energies ($cm^{-1}$) of the $\tilde{A}$ States of Small Peroxy Radicals.

| | $HO_2$ | | $CH_3O_2$ | | *trans* $CH_3CH_2O_2$ | | *gauche* $CH_3CH_2O_2$ | |
|---|---|---|---|---|---|---|---|---|
| Basis set | CIS | DFT | CIS | DFT | CIS | DFT | CIS | DFT |
| 6-31+G(d,p) | 6761 | 8638 | 6572 | 8890 | 6536 | 8938 | 6723 | 9181 |
| 6-311+G(d,p) | 6674 | 8625 | 6564 | 8905 | 6523 | 8945 | 6701 | 9161 |
| 6-311++G(2d,2p) | 7047 | 8690 | 6881 | 8933 | 6805 | 8941 | 7000 | 9186 |
| 6-311++G(2df,2pd) | 7468 | 8811 | 7293 | 9044 | 7220 | 9052 | 7411 | 9282 |
| Experiment | 7029.69[b] | | 7382.8 (.5)[c] | | 7590 (3)[c] | | | |

[a]TD-DFT single points used the CIS/6-31+G(d,p) geometry for the excited state.
[b]Ref. 45.
[c]Ref. 10. Not assigned to a specific conformer.

conformations only causes the computed excitation energies to vary by 700–750 $cm^{-1}$ using CIS and 800–1000 $cm^{-1}$ using TD-DFT. The basis set effects on TD-DFT excitation energies are minimal: 150–200 $cm^{-1}$, being much higher at 6-311++G(2d,2p) than at the smaller basis sets. The differences between the adiabatic and the vertical excitation energies are strongly dependent on the nature of the intramolecular hydrogen bonding in the ground state. Consider the CIS results first: for radicals **I–IV**, which possess hydrogen bonds in their ground states, the difference between the vertical and adiabatic excitation energy (the relaxation energy) is 2025 ± 50 $cm^{-1}$, while the hydrogen bonded conformers of (*Z*)-**V** and (*Z*)-**VI** yield slightly larger relaxation energies: 2467 and 2586 $cm^{-1}$, respectively. By contrast, the non-hydrogen bonded conformers of (*Z*)-**V** and (*Z*)-**VI** and their E isomers (which cannot form intramolecular hydrogen bonds) have much smaller relaxation energies (1280–1464 $cm^{-1}$). These results are consistent with the idea that the hydrogen bonds are very weak in the $\tilde{A}$ state. TD-DFT gives a much different picture of the relaxation energies, which implies different conclusions about the strength of hydrogen bonding in the $\tilde{A}$ state. Relaxation energies calculated at TD-DFT are much smaller, and often negative (vertical excitation energy less than adiabatic). Negative values of the relaxation energy are not physically possible; these likely arise from the fact that the CIS calculations deemphasize intramolecular hydrogen bonding in the $\tilde{A}$ state while hydrogen bonding may still be important to the TD-DFT energies. The groupings of isomers and conformers by relaxation energy are similar to those observed with CIS.

The results described above are clearly seen in Figures 9 and 10. Figure 9 shows the relative adiabatic excitation energies (defined as $T_{ee}$ for a particular isoprene-OH-$O_2$ isomer or conformer minus the lowest value for all isomers and conformers) at TD-DFT vs. CIS. No correlation is evident; instead, there are two groups, one consisting of the hydrogen bonded conformers of (*Z*)-**V** and (*Z*)-**VI**, and the other containing all other isomers. As shown in Figure 10, a plot of the relative *vertical* excitation energies reveals

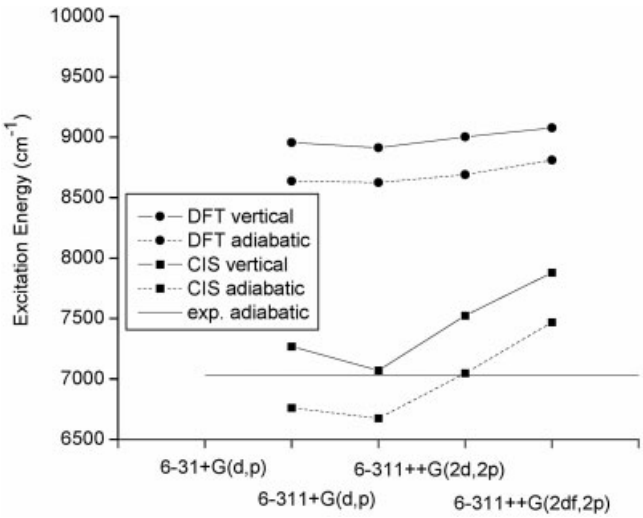


**Figure 6.** Basis set dependence of the vertical and adiabatic excitation energies of $HO_2$, along with the experimental value of the adiabatic excitation energy (straight line).

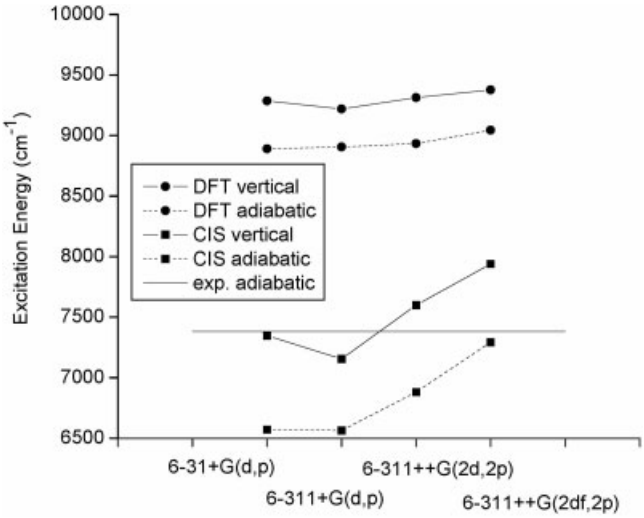


**Figure 7.** Basis set dependence of the vertical and adiabatic excitation energies of $CH_3O_2$, along with the experimental value of the adiabatic excitation energy (straight line).

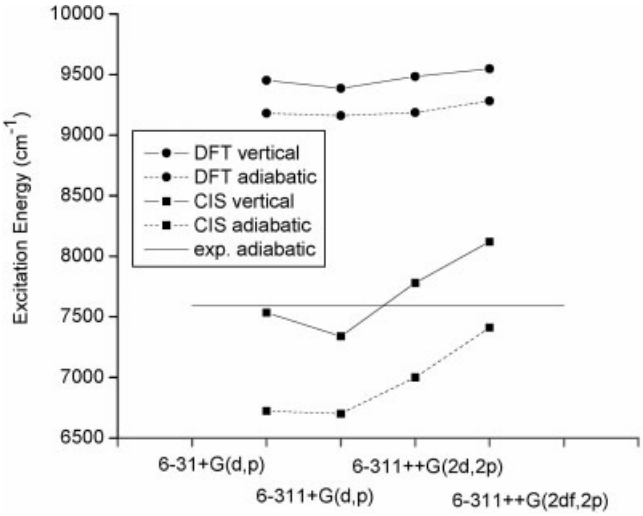


**Figure 8.** Basis set dependence of the vertical and adiabatic excitation energies of *gauche* conformer of $CH_3CH_2O_2$, along with the experimental value of the adiabatic excitation energy (straight line). The plot for the *trans* conformer is very similar.

three well-defined groups that organize themselves by molecular structure and conformation. Figure 10 strongly suggests that both CIS and TD-DFT are providing similarly accurate representations of some aspects of structure affects on excitation energies, while Figure 9 reflects the significantly different treatment of hydrogen bonding in the excited state.

The vibrational frequencies of the Ã state are potentially an important tool for assigning the spectra of the isoprene-OH-$O_2$ radicals. The O—O stretch mode is the dominant progression in the Ã–X̃ transition of the smaller radicals;[11,15,18] therefore, we discuss only computed OO stretch frequencies here. Table 7 reports O—O stretch frequencies of the smaller radicals as a function of basis set. Except for $HO_2$, the computations suggest the existence of a symmetric COO stretch and an asymmetric COO stretch at higher frequency. The computed frequencies are remarkably insensitive to basis set; for $HO_2$, the computed values range from 1091–1123 cm$^{-1}$. Unfortunately, this is much higher than the experimentally determined harmonic stretching frequency of 926.5 ± 2.0 cm$^{-1}$ (by comparison, the MR-CISD study of Langhoff and Jaffe[42] obtained 968 cm$^{-1}$ for the OO stretch frequency of $HO_2$). Unfortunately, computed stretching frequencies are consistently much higher than the experimental values for *all* the radicals for which data is available, but not so consistently that one could derive a reliable scaling factor. It should be noted that the assignments of the bands in the experiments for $CH_3O_2$ and $CH_3CH_2O_2$ are somewhat ambiguous. Molecular structure and conformation have very little affect on the frequency of the asymmetric stretch, although there is a significant affect on the symmetric stretch.

Table 8 reports O—O stretch frequencies of the isoprene-OH-$O_2$ radicals at CIS/6-31+G(d,p). Radical **III** shows only one mode with strong OO stretch character, while the other radicals exhibit at least two modes: one with asymmetric COO stretch character and a symmetric COO stretch mode. Isomers **I** and **IV** of the isoprene-OH-$O_2$ radicals, being identical except for the position of the methyl group, have very similar OO stretch frequencies. The various conformers and isomers of **V** and **VI** yield very

**Table 5.** Vertical and Adiabatic Excitation Energies (cm$^{-1}$) of the $\tilde{A}$ States of Isoprene-OH-$O_2$ Radicals at CIS/6-31+G(d,p).

| Species | Vertical | Adiabatic |
|---|---|---|
| **I** | 8097 | 6026 |
| **II** | 7828 | 5855 |
| **III** | 7822 | 5744 |
| **IV** | 7960 | 5851 |
| (*Z*)-**V** H | 8467 | 6000 |
| (*Z*)-**V** nonH | 7720 | 6256 |
| (*E*)-**V** | 7660 | 6335 |
| (*Z*)-**VI** H | 8347 | 5761 |
| (*Z*)-**VI** nonH | 7725 | 6444 |
| (*E*)-**VI** | 7712 | 6422 |

**Table 6.** Vertical and Adiabatic[a] Excitation Energies (cm$^{-1}$) of the $\tilde{A}$ State of Isoprene-OH-$O_2$ Peroxy Radicals at TD-DFT for Various Basis Sets.

| Species | Basis set | Vertical | Adiabatic |
|---|---|---|---|
| **I** | 6-31+G(d,p) | 9434 | 9233 |
| | 6-311+G(d,p) | 9378 | 9163 |
| | 6-311++G(2d,2p) | 9463 | 9109 |
| **II** | 6-31+G(d,p) | 9420 | 9131 |
| | 6-311+G(d,p) | 9366 | 9055 |
| | 6-311++G(2d,2p) | 9454 | 8993 |
| **III** | 6-31+G(d,p) | 9469 | 9204 |
| | 6-311+G(d,p) | 9416 | 9136 |
| | 6-311++G(2d,2p) | 9511 | 9092 |
| **IV** | 6-31+G(d,p) | 9278 | 9144 |
| | 6-311+G(d,p) | 9231 | 9083 |
| | 6-311++G(2d,2p) | 9314 | 9002 |
| (*Z*)-**V** H | 6-31+G(d,p) | 10081 | 10148 |
| | 6-311+G(d,p) | 10017 | 10102 |
| | 6-311++G(2d,2p) | 10099 | 9956 |
| (*Z*)-**V** nonH | 6-31+G(d,p) | 9549 | 9619 |
| | 6-311+G(d,p) | 9474 | 9535 |
| | 6-311++G(2d,2p) | 9571 | 9491 |
| (*E*)-**V** | 6-31+G(d,p) | 9480 | 9541 |
| | 6-311+G(d,p) | 9407 | 9448 |
| | 6-311++G(2d,2p) | 9504 | 9386 |
| (*Z*)-**VI** H | 6-31+G(d,p) | 10033 | 9720 |
| | 6-311+G(d,p) | 9971 | 9662 |
| | 6-311++G(2d,2p) | 10050 | 9545 |
| (*Z*)-**VI** nonH | 6-31+G(d,p) | 9543 | 9657 |
| | 6-311+G(d,p) | 9462 | 9558 |
| | 6-311++G(2d,2p) | 9557 | 9487 |
| (*E*)-**VI** | 6-31+G(d,p) | 9523 | 9605 |
| | 6-311+G(d,p) | 9442 | 9503 |
| | 6-311++G(2d,2p) | 9540 | 9443 |

[a]TD-DFT single points used the CIS/6-31+G(d,p) geometry for the excited state.

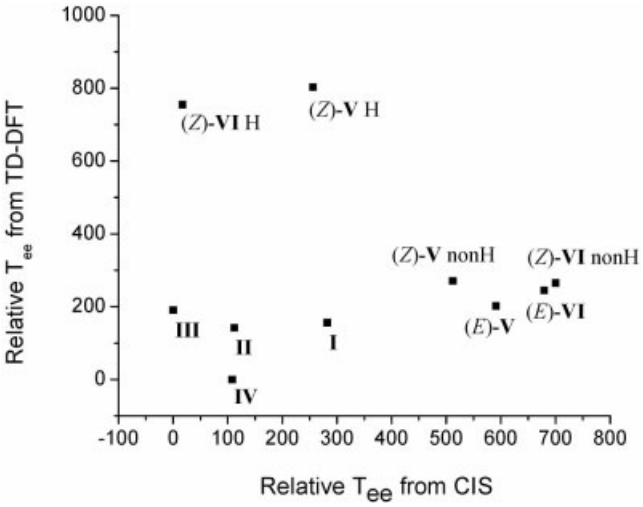


**Figure 9.** TD-DFT vs. CIS relative excitation energies of isoprene-OH-$O_2$ radicals. Adiabatic excitation energies are plotted using the results computed with the 6-31+G(d,p) basis set.

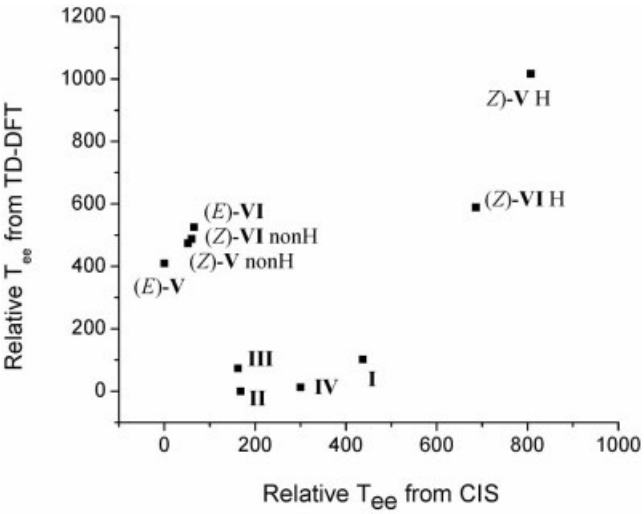


**Figure 10.** TD-DFT vs. CIS relative excitation energies of isoprene-OH-$O_2$ radicals. Vertical excitation energies are plotted using the results computed with the 6-31+G(d,p) basis set.

**Table 8.** $\tilde{A}$ State OO Vibrational Frequencies of Isoprene-OH-$O_2$ Radicals at CIS/6-31+G(d,p).

| Species | Frequency ($cm^{-1}$) |
|---|---|
| **I** | 1105, 1152 |
| **II** | 1157, 1179 |
| **III** | 1011 |
| **IV** | 1087, 1145 |
| (*Z*)-**V** H | 1000, 1148 |
| (*Z*)-**V** nonH | 1000, 1138, 1142 |
| (*E*)-**V** | 986, 1131, 1140 |
| (*Z*)-**VI** H | 991, 1157 |
| (*Z*)-**VI** nonH | 1000, 1146 |
| (*E*)-**VI** | 992, 1122, 1142 |

similar frequencies for the symmetric COO stretch, and distinct similarities among their asymmetric COO stretch frequencies; however, even the latter sets of differences are probably too small to be used to distinguish among these similar species.

## Conclusions

This investigation was initiated in hopes of supporting efforts to assign NIR spectra to different isomers or conformers of the isoprene-OH-$O_2$ radicals using CIS calculations with or without TD-DFT single points. Unfortunately, the results suggest that the transition origins and OO stretch frequencies of these radicals are not terribly sensitive to structure, despite the fact that there are clear groupings based on two different types of structure ($\beta$-hydroxy radicals **I–IV** vs. the $\delta$-hydroxy peroxy radicals) and the presence or absence of hydrogen bonding in the E/Z isomers and conformers of the $\delta$-hydroxy peroxy radicals. Therefore, these modest levels of theory will not help to distinguish or assign NIR spectra of the isomers of these radicals.

## Acknowledgments

The author thanks Renyi Zhang for providing structures of isoprene-OH-$O_2$ radicals, and Joshua Kaplan for assistance with computers and graphics.

**Table 7.** CIS OO Vibrational Frequencies ($cm^{-1}$) of the $\tilde{A}$ State of $HO_2$, $CH_3O_2$, and the *trans* and *gauche* Conformers of $CH_3CH_2O_2$ at Various Basis Sets.

| Species | 6-31+G(d,p) | 6-311+G(d,p) | 6-311++G(2d,2p) | 6-311++G(2df,2pd) | Experiment |
|---|---|---|---|---|---|
| $HO_2$ | 1091 | 1123 | 1114 | 1091 | 926.5[a,b,c] |
| $CH_3O_2$ | 1002, 1172 | 1020, 1186 | 1014, 1175 | 1025, 1188 | 896,[b,d] 1005[d] |
| $CH_3CH_2O_2$ *trans* | 1093, 1152 | 1104, 1167 | 1101, 1158 | 1106, 1171 | |
| $CH_3CH_2O_2$ *gauche* | 1040, 1164 | 1058, 1169 | 1053, 1164 | 1061, 1169 | 918[b,d] |

[a]Ref. 25.
[b]Ref. 21.
[c]Ref. 24.
[d]Ref. 26.

## References


1. Lightfoot, P. D.; Cox, R. A.; Crowley, J. N.; Destriau, M.; Hayman, G. D.; Jenkin, M. E.; Moortgat, G. K.; Zabel, F. Atmos Environ 1992, 26A, 1805.
2. Tyndall, G. S.; Cox, R. A.; Granier, C.; Lesclaux, R.; Moortgat, G. K.; Pilling, M. J.; Ravishankara, A. R.; Wallington, T. J. J Geophys Res 2001, 106, 12157.
3. Cox, R. A.; Coles, J. A. Combust Flame 1985, 60, 109.
4. Warnatz, J. Symp (Int) Combust 1992, 24, 553.
5. Wallington, T. J.; Dagaut, P.; Kurylo, J. J. Chem Rev 1992, 92, 667.
6. Weisman, J. L.; Head–Gordon, M. J. J Am Chem Soc 201, 123, 11686.
7. Elrod, M. J.; Ranschaert, D. L.; Schneider, M. J. Int J Chem Kinet 2001, 33, 363.
8. Zhang, D.; Zhang, R.; North, S. W. J Phys Chem A 2003, 107, 11013.
9. Mah, D. A.; Cabrera, J.; Nation, H.; Ramos, M.; Sharma, S.; Nickolaisen, S. L. J Phys Chem A 2003, 107, 4354.
10. Pushkarsky, M. B.; Zalbuovsky, S. J.; Miller, T. A. J Chem Phys 2000, 112, 10695.
11. Atkinson, D. B.; Spillman, J. L. J Phys Chem A 2002, 106, 8891.
12. Deev, A.; Powers, D. N.; Sommar, J.; Okumura, M.; Ohio State University, 58th International Symposium on Molecular Spectroscopy, Columbus, OH, 2004.
13. Zalyubovsky, S. J.; Glover, B. G.; Miller, T. A.; Hayes, C.; Merle, J. K.; Hadad, C. M. J Phys Chem A, 2004, 109, 1308.
14. Frost, J. F.; Ellison, G. B.; Vaida, V. J Phys Chem A 1999, 103, 10169.
15. Guenther, A.; Hewitt, C. N.; Erickson, D.; Fall, R.; Geron, C.; Graedel, T.; Harley, P.; Klinger, L.; Lerdau, M.; McKay, W. A.; Pierce, T.; Scholes, B.; Steinbrecher, R.; Tallamraju, R.; Taylor, J.; Zimmerman, P. J Geophys Res 1995, 100, 8873.
16. Paulson, S. E.; Seinfeld, J. H. J Geophys Res 1992, 97, 20703.
17. Dibble, T. S. J Phys Chem A 2002, 106, 6643.
18. Geiger, H.; Barnes, I.; Bejan, I.; Benter, T.; Spittler, M. Atmos Environ 2003, 37, 1503.
19. Stevens, P. S.; Mather, J. H.; Brune, W. H.; Eisele, F.; Tanner, D.; Jefferson, A.; Cantrell, C.; Shetter, R.; Sewall, S.; Fried, A.; Henry, B.; Williams, E.; Baumann, K.; Goldan, P.; Kuster, W. J Geophys Res D 1997, 102, 6379.
20. Poschl, U.; von Kuhlmann, R.; Roisson, N.; Crutzen, P. J. J Atmos Chem 2000, 37, 29.
21. Hunziker, H. E.; Wendt, H. R. J Chem Phys 1976, 64, 3488.
22. Becker, K. H.; Fink, E. H.; Leiss, A.; Schurath, U. Chem Phys Lett 1978, 54, 191.
23. Freedman, P. A. Faraday Trans II 1976, 72, 207.
24. Ramond, R. M.; Blanksby, S. J.; Kato, S.; Bierbaum, V. M.; Davico, G. E.; Schwartz, R. L.; Lineberger, W. C.; Ellison, G. B. J Phys Chem A 2002, 106, 9841.
25. Holstein, K. J.; Fink, E. H.; Zabel, F. J. Mol Spectrosc 1983, 99, 231.
26. Blanksby, S. J.; Ramond, T. M.; Davico, G. E.; Mimlos, M. R.; Kato, S.; Bierbaum, V. M.; Lineberger, W. C.; Ellison, G. B.; Okumura, M. J Am Chem Soc 2001, 123, 9585.
27. Frisch, M. J.; Trucks, G. W.; Schlegel, H. B.; Scuseria, G. E.; Robb, M. A.; Cheeseman, J. R.; Zakrzewski, V. G.; Montgomery, J. A., Jr.; Stratmann, R. E.; Burant, J. C.; Dapprich, S.; Millam, J. M.; Daniels, A. D.; Kudin, K. N.; Strain, M. C.; Farkas, O.; Tomasi, J.; Barone, V.; Cossi, M.; Cammi, R.; Mennucci, B.; Pomelli, C.; Adamo, C.; Clifford, S.; Ochterski, J.; Peterson, G. A.; Ayala, P. Y.; Cui, Q.; Morokuma, K.; Malick, D. K.; Rabuck, A. D.; Ragahavachari, K.; Foresman, J. B.; Cioslowski, J.; Ortiz, J. V.; Stefanov, B. B.; Liu, G.; Liashenko, A.; Piskorz, P.; Komaromi, I.; Gomperts, R.; Martin, R. L.; Fox, D. J.; Keith, T.; Al-Laham, M. A.; Peng, C. Y.; Nanayakkara, A.; Gonzalez, C.; Challacombe, M.; Gill, P. M. W.; Johnson, B.; Chen, W.; Wong, M. W.; Andres, J. L.; Gonzalez, C.; Head–Gordon, M.; Replogle, E. S.; Pople, J. A. Gaussian 98, revision A.6; Gaussian, Inc.: Pittsburgh, PA, 1998.
28. Boyd, S. L.; Boyd, R. J.; Barclay, L. R. J Am Chem Soc 1990, 112, 5724.
29. Quelch, G. E.; Gallo, M. M.; Schaefer, H. F., III. J Am Chem Soc 1990, 112, 5724.
30. Reintstra–Kiracofe, J. C.; Allen, W. D.; Schaefer, H. F., III. J Phys Chem A 2000, 104, 9823.
31. Becke, A. D. J Chem Phys 1993, 98, 5648.
32. Lee, C.; Yang, W.; Parr, R. G. Phys Rev B 1988, 37, 785.
33. Byrd, E. F. C; Sherrill, C. D.; Head–Gordon, M. J Phys Chem A 2001, 105, 9736.
34. Lei, W.; Zhang, R.; McGivern, W. S.; Dereskei–Kovacs, A.; North, S. W. J Phys Chem A 2001, 105, 471.
35. Runge, E.; Gross, E. K. U. Phys Rev Lett 1984, 52, 997.
36. Strattman, R. E.; Scuseria, G. E.; Frisch, M. J. J Chem Phys 1998, 109, 8218.
37. Petersilka, M.; Gossmann, U.; Gross, E. K. U. Phys Rev Lett 1996, 76, 1212.
38. Bauernschmitt, R.; Ahlrichs, R. Chem Phys Lett 1996, 256, 454.
39. Stanton, J. F.; Gauss, J.; Ishikawa, N.; Head–Gordon, M. J Chem Phys 1995, 103, 4160.
40. Grana, A. M.; Lee, T. J.; Head–Gordon, M. J Phys Chem 1995, 99, 3493.
41. Tuckett, R. P.; Freedman, P. A.; Jones, W. J. Mol Phys 1979, 37, 403.
42. Langhoff, S. R.; Jaffe, R. L. J Chem Phys 1979, 71, 1485.
43. Aloisio, S.; Li, Y.; Francisco, J. S. J Chem Phys 1999, 110, 9017.
44. Fink, E. H.; Ramsay, D. A. J Mol Spectros 1997, 185, 304.